

Evidence for transfer followed by breakup in ${}^7\text{Li} + {}^{65}\text{Cu}$

A. Shrivastava^{a *}, A. Navin^{a†}, N. Keeley^b, K. Mahata^a, K. Ramachandran^a, V. Nanal^c, V.V. Parkar^a, A. Chatterjee^a and S. Kailas^a

^aNuclear Physics Division, Bhabha Atomic Research Centre, Mumbai 400085, India

^bDSM/DAPNIA/SPhN, CEA Saclay, F-91191 Gif sur Yvette, France

^cDNAP, Tata Institute of Fundamental research, Mumbai 400005, India

The observation of a large cross-section for the $\alpha + d$ channel compared to breakup into the $\alpha + t$ channel from an exclusive measurement for the ${}^7\text{Li} + {}^{65}\text{Cu}$ system at 25 MeV is presented. A detailed analysis of the angular distribution using coupled channels Born approximation calculations has provided clear evidence that the observed $\alpha + d$ events arise from a two step process, i.e. direct transfer to the 2.186 MeV (3^+) resonance in the $\alpha + d$ continuum of ${}^6\text{Li}$ followed by breakup, and are not due to final state interaction effects.

PACS: 25.70.Mn, 25.70.Hi, 25.70.Bc, 25.70.Ef, 24.10.Eq

Keywords: Exclusive breakup, Transfer-breakup, Elastic scattering, Weakly bound nuclei, Coupled channels calculations.

*email:aradhana@apsara.barc.ernet.in

†Permanent address: GANIL, Bd. Henri Becquerel, BP 55027, Cedex 5, 14076, Caen, France

1. Introduction

Nuclear reactions involving unstable/weakly bound nuclei that have low breakup thresholds and exotic structures display features remarkably different from those of well-bound stable nuclei. The advent of recent ISOL facilities, apart from opening new avenues in this field, has also caused a revival in the study of stable but weakly bound nuclei like ${}^6,{}^7\text{Li}$ and ${}^9\text{Be}$. Measurements with these nuclei, with better understood cluster structures, are relatively easier, due to the larger available beam intensities. At energies around the barrier the effect of breakup on the fusion process and also the measurement of associated direct processes are topics of current interest.

Recent interpretations of measurements of products arising from the excited compound nucleus (fission or evaporation residues) show the need for distinguishing between various mechanisms leading to the same final product prior to deriving any conclusions about the effect of weak binding on other reaction processes [1,2]. Measurements involving ${}^6\text{He}$ and ${}^6,{}^7\text{Li}$ [2,3,4,5,6], having an alpha + x configuration, show significantly large cross-sections for alpha particle production. It is non-trivial to disentangle the contributions to the alpha yield arising from different reaction mechanisms that include fusion-evaporation, transfer, transfer followed by evaporation/ breakup of the ejectile and direct (non capture) breakup of the projectile, especially from inclusive measurements. It is a well known observation that the alpha yield is much larger than the corresponding triton/deuteron yield in reactions involving ${}^6,{}^7\text{Li}$ beams and some possible scenarios have been suggested [7,8,9,10,11].

Exclusive measurements of alpha particles provide a tool to understand the deconvolution of these processes. Such measurements, along with differential cross-sections for various direct processes like elastic scattering and few nucleon transfer reactions, provide important constraints for coupled channels calculations necessary for a consistent understanding of reactions with weakly bound nuclei near the Coulomb barrier. Apart from the above stated motivations, one of the key aspects of the present work is to investigate the two step reaction mechanism, namely, one nucleon transfer to a resonant state followed by breakup, for the case of a ${}^7\text{Li}$ projectile. This complex process needs the simultaneous understanding of both the breakup and transfer reactions. Further, such measurements also provide information on the ${}^7\text{Li}$ wave function in terms of the ${}^6\text{Li}(\text{ground/resonance})+n$ configuration. In an earlier measurement for the ${}^7\text{Li}+{}^{197}\text{Au}$ system [12], the authors speculated on the possibility of such a process and placed limits on the cross-section. Recently, analysing powers for this type of reaction have been reported [13]. In more recent exclusive measurements of $\alpha - n$ for the ${}^6\text{He} + {}^{209}\text{Bi}$ system, the contributions of single and two neutron transfer to the continuum followed by evaporation have been reported [14,15]. The present work is the first quantitative measurement of differential cross-section for the transfer-breakup reaction.

We report in this letter exclusive measurements of alpha particles along with d/t to identify different reaction mechanisms of alpha emission, and a detailed study of the transfer-breakup mechanism of ${}^7\text{Li}$ on a medium mass target at energies near the Coulomb barrier. These have been compared with similar measurements using a ${}^6\text{Li}$ beam. Elastic scattering angular distributions and nucleon transfer angular distributions have also been measured. Extensive coupled channels Born approximation (CCBA) calculations along

with continuum discretized coupled channels calculations (CDCC) to simultaneously explain the large number of observables are presented.

2. Experimental details and results

The measurements were performed at the 14UD BARC-TIFR Pelletron, Mumbai using 25 MeV ${}^6,7\text{Li}$ beams on an enriched ${}^{65}\text{Cu}$ target. The target thickness used for measuring the elastic scattering and nucleon-transfer differential cross-sections was 1.0 mg/cm^2 , while for the exclusive breakup it was 2.5 mg/cm^2 . Typical beam currents were around 2 pA. The coincidence detection system consisted of three $\Delta E(30, 40\text{ and }47\mu\text{m})\text{-E}(2\text{mm})$ Si surface barrier telescopes and a $10 \times 10 \times 10\text{mm}^3$ CsI(Tl) charged particle detector, kept 20° apart. With the present setup it was possible to measure fragment kinetic energies corresponding to unbound states of ${}^6,7\text{Li}$ up to an excitation energy of 5.5 MeV. From the measured kinetic energy of each fragment and the breakup Q value, the relative energies between $\alpha\text{-}d(t)$ for ${}^6\text{Li}({}^7\text{Li})$ breakup were deduced using three body final state correlations [16]. The detectors were calibrated using discrete energy alpha particles in the range of 12 to 26 MeV [17], produced in the reaction with ${}^7\text{Li}$ beam of energies 20 and 25 MeV on a $50\text{ }\mu\text{g/cm}^2$ thick ${}^{12}\text{C}$ target. The elastic scattering, transfer and alpha emission angular distribution measurements were performed in a separate experiment employing three Si-surface barrier telescopes ($\Delta E\text{- }10, 20\text{ and }25\text{ }\mu\text{m}$ and $E\text{- }1\text{mm}$) covering an angular range of 10° to 140° . A $300\text{ }\mu\text{m}$ thick Si- detector at forward angles, for both the exclusive and inclusive measurements, was used for monitoring the number of incident beam particles.

The data were collected in an event by event mode, with the trigger generated from fast coincidences between adjacent detectors. In Fig. 1 alpha and deuteron coincidence spectra for both the systems at $\theta_{\alpha d} = 20^\circ$ are shown. The two localized contributions in the spectra are identified using three body kinematics [16], and correspond to the sequential breakup of the first resonant state in ${}^6\text{Li}$. The full curves in Figs. 1a and 1b show the calculated kinematic correlations for the breakup of the 3^+ state in ${}^6\text{Li}$. In Fig. 1b, the relative energy ($E_{\alpha d}$) of 0.71 corresponding to the 3^+ resonance state is indicated. Fig. 1c shows the projection of Fig. 1b along the alpha energy axis. The alpha particles moving forward (backward) in the $\alpha\text{-}d$ center of mass system corresponds to the high (low) energy peak in the spectrum.

Shown in Fig. 2a are the angular distributions for the breakup of ${}^6\text{Li}$ proceeding through the 3^+ and 2^+ resonant states at 2.186 and 4.312 MeV, respectively. Differential cross-sections were computed from $\alpha + d$ coincidence yields, assuming isotropic emission of breakup fragments in the ${}^6\text{Li}^*$ frame and are shown in Fig. 2. The Jacobian of transformation and the center of mass angle of the scattered ${}^6\text{Li}^*$ were obtained as described in references [18,19]. The ground state and first resonant state (3^+ , 2.186 MeV) of ${}^6\text{Li}$ are well described with a $\alpha + d$ configuration [20]. The decay of the second resonant state (0^+ , 3.56 MeV) of ${}^6\text{Li}$ to $\alpha + d$ is forbidden due to parity considerations; however, a decay through the $t + {}^3\text{He}$ channel is possible. The cross-section for this state was inferred to be negligible as ${}^3\text{He} + t$ coincidences were not observed.

The importance of the two step process can be seen from Fig. 1d which shows the $\alpha + d$ coincidences for the ${}^7\text{Li}+{}^{65}\text{Cu}$ system at 25 MeV. Two clear peaks are seen in the deuteron vs alpha energy correlation plot, indicating breakup of ${}^6\text{Li}$ formed after one

neutron stripping ($Q = -0.185$ MeV) of ${}^7\text{Li}$ and clearly not breakup of ${}^7\text{Li}$ into $\alpha + d + n$ ($Q = -8.8$ MeV). From the relative energy plot shown in Fig. 1e, the two peaks can be identified as arising from the breakup of ${}^6\text{Li}$ via its 2.18 MeV state, formed after a one neutron transfer reaction. The transferred neutron can populate various states in ${}^{66}\text{Cu}$ depending on their spin and spectroscopic factors. The kinematic curves shown in the figure are for transfer of the neutron to the ground, 1.15 MeV and 2.14 MeV states of ${}^{66}\text{Cu}$ with ${}^6\text{Li}$ in its 3^+ resonance state. As can be seen from the figure, there is very good agreement of the data with these kinematic plots. The corresponding angular distribution, integrated over excited states of ${}^{66}\text{Cu}$, is displayed in Fig. 2b. Also shown in the figure are the angular distributions for the breakup of ${}^7\text{Li} \rightarrow \alpha + t$ through its first resonance state at 4.63 MeV. From the known cluster structure of ${}^7\text{Li}$ one would have naively expected a much larger cross-section for the latter compared to the $\alpha + d$ coincidence yield.

The measured elastic angular distributions for the ${}^6\text{Li} + {}^{65}\text{Cu}$ and ${}^7\text{Li} + {}^{65}\text{Cu}$ systems are shown in Figs. 2c and 2d, respectively. The errors on the data points shown in the figure are statistical only. The angular distribution for the one neutron stripping of ${}^7\text{Li} + {}^{65}\text{Cu}$ ($Q = -0.185$ keV) populating ${}^6\text{Li}$ in its ground state (as ${}^6\text{Li}$ has no bound excited states) and ${}^{66}\text{Cu}$ (E^* up to 5 MeV) was obtained independently from the inclusive data. The integrated cross-section obtained assuming a Gaussian shape for the angular distribution is listed in Table 1. As can be seen from Table 1, this cross-section is larger than that for all the other direct processes listed. The errors on the measured cross-sections are from uncertainties in the fitting procedure (6 to 8%) and statistics (3 to 6%). The $1n$ -pickup and t -stripping cross-section for ${}^6\text{Li} + {}^{65}\text{Cu}$ are also listed in Table 1. For both isotopes the exclusive breakup cross-section is observed to be much smaller than the inclusive cross-section for alpha emission. The contribution of alpha particles evaporated from the compound nucleus is estimated to be less than 30% (Table 1) of the total inclusive alpha yield. These were obtained by fitting the measured backward angle alpha angular distribution using the statistical model code PACE [21]. This suggests that the majority of the alpha particle yields arise from processes where the deuteron (triton) is transferred or captured by the target [7,8,9,10,11] after breakup of the ${}^6\text{Li}({}^7\text{Li})$ in field of the target. The alpha emission cross-section from the inclusive and exclusive data for the ${}^6\text{Li}$ projectile is larger than that for ${}^7\text{Li}$, as expected from the difference in the breakup thresholds. Similar results for the inclusive alpha emission cross-sections for ${}^6\text{Li}$ and ${}^7\text{Li}$ were obtained in references [6,22].

3. Calculations

Two distinct sets of calculations were carried out to describe the data. Those for the elastic scattering and breakup processes were performed within the CDCC formalism using a cluster folding model [23] for the structure of ${}^{6,7}\text{Li}$. Calculations for the transfer breakup employed the CCBA framework, i.e. CDCC in the entrance and exit channel and DWBA for the transfer step, utilizing the potentials that explained the elastic scattering data. Both the CCBA and CDCC calculations described here were performed using the code FRESKO [24].

The CDCC calculations for ${}^6\text{Li}$ (${}^7\text{Li}$) were similar to those described in [25,26] and assumed an $\alpha+d(t)$ cluster structure. The binding potentials between $\alpha+d$ and $\alpha+t$ were

taken from [27] and [28], respectively. The $\alpha+d(t)$ continuum was discretized into a series of momentum bins of width $\Delta k = 0.2 \text{ fm}^{-1}$ (up to $k = 0.8 \text{ fm}^{-1}$) for $L = 0, 1, 2$ for ${}^6\text{Li}$ and $L = 0, 1, 2, 3$ for ${}^7\text{Li}$, where $\hbar k$ denotes the momentum of the $\alpha + d(t)$ relative motion. All couplings, including continuum–continuum couplings, up to multipolarity $\lambda = 2$ were incorporated. Optical potentials for $\alpha+{}^{65}\text{Cu}$ and $d(t)+{}^{65}\text{Cu}$ are required as input for the cluster-folded ${}^6\text{Li}({}^7\text{Li})+{}^{65}\text{Cu}$ potential. The potential for $\alpha+{}^{65}\text{Cu}$ was obtained by adjusting the real and imaginary depths of the global α optical potential of Avrigeanu *et al.* [29], in order to match the measured $\alpha+{}^{65}\text{Cu}$ elastic scattering data of reference [30]. In the absence of suitable elastic scattering data, the global parameters of [31,32] were employed for the $t+{}^{65}\text{Cu}$ and $d+{}^{65}\text{Cu}$ optical potentials. The real and imaginary strengths of the cluster-folded potentials were adjusted to describe the elastic scattering data.

Results of the calculations for the elastic scattering are shown in Figs. 2c and 2d. The two different curves are results of the calculation performed with (solid lines) and without (dashed lines) couplings. The calculated angular distributions for the resonant states, 3^+ and 2^+ of ${}^6\text{Li}$ (Fig. 2a) and $7/2^-$ of ${}^7\text{Li}$ (Fig. 2b) show good agreement with the data. The results of the full CDCC calculation are listed in Table 1. The angle integrated cross-sections of the resonant states obtained by fitting to a Gaussian distribution show good agreement with the calculation. The total calculated breakup cross-sections for ${}^6\text{Li}$ and ${}^7\text{Li}$ were obtained by integrating contributions from the states in the continuum up to 11 MeV. As can be seen in Table 1, the total ${}^7\text{Li}({}^6\text{Li}) \rightarrow \alpha + t(d)$ breakup provides a negligible contribution to the total reaction cross-section. The fusion cross-sections listed in Table 1, for ${}^{6,7}\text{Li} + {}^{65}\text{Cu}$ were obtained using the barrier penetration model, as described in reference [33].

As mentioned earlier, for the ${}^7\text{Li} + {}^{65}\text{Cu}$ system a significant number of $\alpha+d$ coincidence events consistent with decay of the 2.18 MeV ${}^6\text{Li}(3^+)$ resonance were observed. The simplest reaction mechanism for producing these events is a transfer–breakup process, with direct neutron stripping to the unbound 3^+ resonance and/or neutron stripping to the ${}^6\text{Li}$ 1^+ ground state followed by excitation to the 3^+ resonance through final state interaction. Due to the high density of states in the residual ${}^{66}\text{Cu}$ nucleus and the experimental resolution, the angular distribution of ${}^6\text{Li}(3^+)$ resonance events was integrated over the residual ${}^{66}\text{Cu}$ excitation energy up to 2.5 MeV. The ${}^{66}\text{Cu}$ could thus be left in any one of up to 40 states [34].

It was not possible to incorporate this process directly into the full CDCC calculation. Thus, to establish the dominant reaction mechanism for the observed $\alpha+d$ coincidences in ${}^7\text{Li} + {}^{65}\text{Cu}$ (direct transfer to the continuum or transfer to ground state followed by breakup), a series of CCBA calculations employing a much reduced coupling scheme in the entrance and exit partitions, shown in Fig. 3 was performed. The potentials used were taken from the CDCC calculation as explained in the previous paragraph. For the ${}^6\text{Li}+{}^{66}\text{Cu}$ exit partition, only coupling to the 2.18 MeV (3^+) of ${}^6\text{Li}$ was retained. The optical potential for $\alpha+{}^{66}\text{Cu}$ was again calculated from the global parameters of Avrigeanu *et al.* [29], renormalized by the same factors needed to fit the 14 MeV $\alpha+{}^{66}\text{Cu}$ data of Costa *et al.* [30]. The optical potential for $d+{}^{66}\text{Cu}$ was the central part of the potential of Bieszk and Knutson [35] for 9 MeV $d+{}^{63}\text{Cu}$. Spectroscopic factors for the ${}^7\text{Li} \rightarrow {}^6\text{Li}+n$ overlaps were taken from Cohen and Kurath [36]. The neutron was bound in a Woods–Saxon well

of radius $1.25 \times A^{1/3}$ fm and diffuseness 0.65 fm, the depth being adjusted to yield the correct binding energy. The spectroscopic factors for ${}^{66}\text{Cu} \rightarrow {}^{65}\text{Cu}+n$ were taken from Daehnick and Park [34]. The neutron was again bound in a Woods–Saxon well of radius $1.25 \times A^{1/3}$ fm and diffuseness 0.65 fm, as used in ref. [34]. The transfer part of the calculations was performed using the post-form DWBA and included the full complex remnant term.

The CCBA calculations were carried out for transfers leaving the residual ${}^{66}\text{Cu}$ in levels up to 1.43 MeV in excitation, partly due to the uncertain nature of many of the spin assignments above 1.5 MeV and the presence of unresolved doublets. As the reaction Q-value for ${}^{65}\text{Cu}({}^7\text{Li}, {}^6\text{Li}){}^{66}\text{Cu}$ is slightly negative (-0.185 MeV), the population of states near the ground state of ${}^{66}\text{Cu}$ will be favoured to some extent due to Q-matching considerations. Hence the sum of the present CCBA calculations covers most of the observed $\alpha+d$ coincidence cross-section. In the cases where the spin assignments of Daehnick and Park differ from those of the compilation [37], the latter has been followed. The shape of the calculated sum of the CCBA angular distributions is in good agreement with the measurement (Fig. 2b), although the magnitude is lower due to the omission of ${}^{66}\text{Cu}$ states above 1.43 MeV. The results of the calculation confirm the transfer/breakup mechanism for the observed $\alpha+d$ coincidences. Normalising the summed CCBA calculations to the data yields a total cross-section for ${}^6\text{Li}(3^+)$ production of about 9 mb, nearly twice that for the measured breakup of ${}^7\text{Li}$ via $7/2^-$ state. The separately measured ${}^{65}\text{Cu}({}^7\text{Li}, {}^6\text{Li}){}^{66}\text{Cu}$ reaction leaving ${}^6\text{Li}$ in its ground state is also well described. The dominant peak in the spectrum for this transfer is centred on the 1.15 MeV 6^- state in ${}^{66}\text{Cu}$, and the experimental value for the total cross section integrated over a bin of width 400 keV centred at 1.15 MeV is 4.2 ± 0.5 mb, while the summed total cross section from the CCBA calculation for ${}^{66}\text{Cu}$ states in the same energy range is 3.9 mb.

Having established that the ${}^6\text{Li}(3^+)$ resonance is populated by the transfer–breakup mechanism, a further distinction between direct transfer to the unbound 3^+ resonance in ${}^6\text{Li}$ (transfer to the continuum) and transfer to ${}^6\text{Li}$ in its 1^+ ground state followed by excitation to the 3^+ (final state interaction) was investigated. Calculations omitting the direct transfer step showed that the final state interaction process provides a negligible contribution (10%) except at extreme forward angles. It can thus be concluded that the main reaction mechanism for the observed large $\alpha + d$ exclusive cross-sections is direct transfer followed by breakup of the unbound 3^+ resonant state in the ${}^6\text{Li}$ continuum.

4. Discussion

The exclusive breakup cross-sections for the resonant states of ${}^{6,7}\text{Li}$ could be explained well by CDCC calculations performed using potentials that fit the elastic scattering angular distributions. The total non capture breakup cross-section for ${}^6\text{Li}$ was found to be larger than that for ${}^7\text{Li}$ mainly due to the lower alpha binding energy in ${}^6\text{Li}$ compared to ${}^7\text{Li}$. The exclusive breakup cross-sections are a very small fraction of the reaction cross-sections for both ${}^6\text{Li}$ and ${}^7\text{Li}$ (Table 1). The exclusive breakup for ${}^{6,7}\text{Li} + {}^{65}\text{Cu}$ contributes less than 10% and compound nucleus evaporation less than 30% towards the observed large alpha-singles cross-section. The origin of the large alpha yield in ${}^6\text{Li}({}^7\text{Li})$ induced reactions seems to be mainly due to deuteron(triton) capture/deuteron(triton)

transfer as discussed in [7,8,9,10,11].

In a recent study with ${}^6,7\text{Li}$ on a medium mass target, ${}^{64}\text{Zn}$, very large cross-sections for the breakup (where both the fragments survive) have been indirectly inferred by subtracting the complete and incomplete fusion cross-sections from the reaction cross-section [38]. This could arise from a neglect of other direct reaction processes, for instance; nucleon transfer, inelastic excitation of the target/projectile etc. Before arriving at any conclusion on the role of breakup on other reaction channels unambiguous information on the breakup cross-section is necessary. The present work clearly shows that exclusive measurements for the breakup cross-sections are essential and indirect methods can be unreliable.

5. Conclusion

The present work reports a detailed study of the multi-step reaction mechanism, namely transfer-breakup. The origin of the large yields for $\alpha + d$ events from the coincidence data for ${}^7\text{Li}$ breakup has been identified as transfer followed by breakup of the excited ${}^6\text{Li}$ via its 3^+ resonant state in the continuum. To get a deeper insight into the mechanism behind this reaction – direct transfer of the neutron to the ${}^6\text{Li}$ -continuum or transfer to the ground state of ${}^6\text{Li}$ followed by excitation to the continuum – CCBA calculations were performed. The results of the calculations have established that the main reaction mechanism is direct transfer to the continuum.

Reactions with low energy unstable radioactive ion beams from newly available facilities are expected to be of similar complexity. Identification of the reaction processes and development of theoretical understanding for such multi-step reactions is a challenging task. The present study with weakly bound stable nuclei on breakup and transfer–breakup mechanism along with extensive theoretical analysis is an attempt in this direction.

REFERENCES

1. R. Raabe, *et al.*, Nature 431 (2004) 823, and references therein.
2. A. Navin, *et al.*, Phys. Rev. C 70 (2004) 044601.
3. A. di Pietro, *et al.*, Europhys. Lett. 64 (2004) 309.
4. A. Pakou, *et al.*, Phys. Rev. Lett. 90 (2003) 202701.
5. J.J. Kolata, Eur. Phys. J. A 13 (2002) 117.
6. G.R. Kelly, *et al.*, Phys. Rev. C 63 (2000) 024601.
7. V. Tripathi, *et al.*, Phys. Rev. C 72 (2005) 0170601.
8. C. Signorini, *et al.*, Phys. Rev. C 67 (2003) 044607.
9. C. M. Castaneda, *et al.*, Phys. Lett. B 77 (1978) 371.
10. J.G. Fleissner, *et al.*, Phys. Rev. C 17 (1978) 1001.
11. H. Utsunomiya, *et al.*, Phys. Rev. C 28 (1983) 1975.
12. J.L. Quebert, *et al.*, Phys. Rev. Lett. 32 (1974) 1136.
13. N. Davis, *et al.*, Phys. Rev. C 69 (2004) 064605.
14. J.P. Bychowski, *et al.*, Phys. Lett. B 596 (2004) 26.
15. P.A. DeYoung, *et al.*, Phys. Rev. C 71 (2005) 051601.
16. D. Scholz, *et al.*, Nucl. Phys. A 288 (1977) 351.
17. I. Tserruya, B. Rosner and K. Bethge, Nucl. Phys. A 213 (1973) 22.

18. R.J.de. Meijer and R. Kamermans, *Rev. Mod. Phys.* 57 (1985) 147.
19. H. Fuchs, *Nucl. Instr. and Meth.* 190 (1981) 75.
20. D.R. Tilley, *et al.*, *Nucl. Phys. A* 708 (2002) 3.
21. A. Gavron, *Phy. Rev. C* 21 (1980) 230.
22. K.O. Pfeiffer, *et al.*, *Nucl. Phys. A* 206 (1973) 545.
23. B. Buck and A.A. Pilt, *Nucl. Phys. A* 280 (1977) 133.
24. I.J. Thompson, *Comp. Phys. Rep.* 7 (1988) 167.
25. N. Keeley, *et al.*, *Phys. Rev. C* 68 (2003) 054601.
26. N. Keeley, K.W. Kemper, and K. Rusek, *Phys. Rev. C* 66 (2002) 044605.
27. K.-I. Kubo and M. Hirata, *Nucl. Phys. A* 187 (1972) 186.
28. B. Buck and A.C. Merchant, *J. Phys. G* 14 (1988) L211.
29. V. Avrigeanu, P.E. Hodgson, and M. Avrigeanu, *Phys. Rev. C* 49 (1994) 2136.
30. S. Costa, *et al.*, *Nuovo Cim.* 72 A (1982) 40.
31. F.D. Becchetti, Jr. and G.W. Greenlees, *Polarization Phenomena in Nuclear Reactions* (H.H. Barschall and W. Haerberli, eds.) p. 682, The University of Wisconsin Press, Madison, Wis. (1971); C.M. Perey and F.G. Perey, *Atomic Data and Nucl. Data Tables* 17 (1976) 1.
32. C.M. Perey and F.G. Perey, *Phys. Rev.* 132 (1963) 755; C.M. Perey and F.G. Perey, *Atomic Data and Nucl. Data Tables* 17 (1976) 1.
33. N. Keeley, K.W. Kemper and K. Rusek, *Phys. Rev. C* 65 (2002) 014601.
34. W.W. Daehnick and Y.S. Park, *Phys. Rev.* 180 (1969) 1062.
35. J.A. Bieszk and L.D. Knutson, *Nucl. Phys. A* 349 (1980) 445.
36. S. Cohen and D. Kurath, *Nucl. Phys. A* 101 (1967) 1.
37. M.R. Bhat, *Nucl. Data Sheets* 83 (1998) 789.
38. P.R.S. Gomes, *et al.*, *Phys. Lett B* 601 (2004) 20; P.R.S. Gomes *et al.*, *Phy. Rev. C* 71 (2005) 034608.

Table 1

Cross-sections for various channels in ${}^6\text{Li} + {}^{65}\text{Cu}$ and ${}^7\text{Li} + {}^{65}\text{Cu}$ systems. The calculated values are result of coupled channel calculations (see text).

${}^6\text{Li} + {}^{65}\text{Cu}$		
Channel	σ_{exp} (mb)	σ_{cal} (mb)
${}^6\text{Li}^*(2.186 \text{ MeV}) \rightarrow \alpha + d$	22 ± 2	19.5
${}^6\text{Li}^*(4.31 \text{ MeV}) \rightarrow \alpha + d$	4.3 ± 0.5	3.9
${}^6\text{Li}^*(5.65 \text{ MeV}) \rightarrow \alpha + d$	-	0.8
${}^6\text{Li}^*(\text{upto } 11 \text{ MeV}) \rightarrow \alpha + d$	-	48
${}^7\text{Li}$ (1-neutron pickup)	14.7 ± 2.0	-
${}^3\text{He}$ (triton stripping)	3.3 ± 0.5	-
α (CN evaporation)	177 ± 20	-
α (inclusive)	612 ± 40	-
Fusion	-	1199
Total reaction	-	1492
${}^7\text{Li} + {}^{65}\text{Cu}$		
Channel	σ_{exp} (mb)	σ_{cal} (mb)
${}^7\text{Li}^*(4.652 \text{ MeV}) \rightarrow \alpha + t$	4.5 ± 0.6	5.1
${}^7\text{Li}^*(7.454 \text{ MeV}) \rightarrow \alpha + t$	-	0.4
${}^7\text{Li}^*(\text{upto } 11 \text{ MeV}) \rightarrow \alpha + t$	-	20.9
${}^6\text{Li}^*(2.186 \text{ MeV}) \rightarrow \alpha + d$	9 ± 1	5.6
${}^6\text{Li}$ (1-neutron stripping)	44 ± 4	9.3
${}^6\text{He}$ (1-proton stripping)	7.8 ± 1.0	-
α (CN evaporation)	110 ± 18	-
α (inclusive)	422 ± 33	-
Fusion	-	1061
Total reaction	-	1401

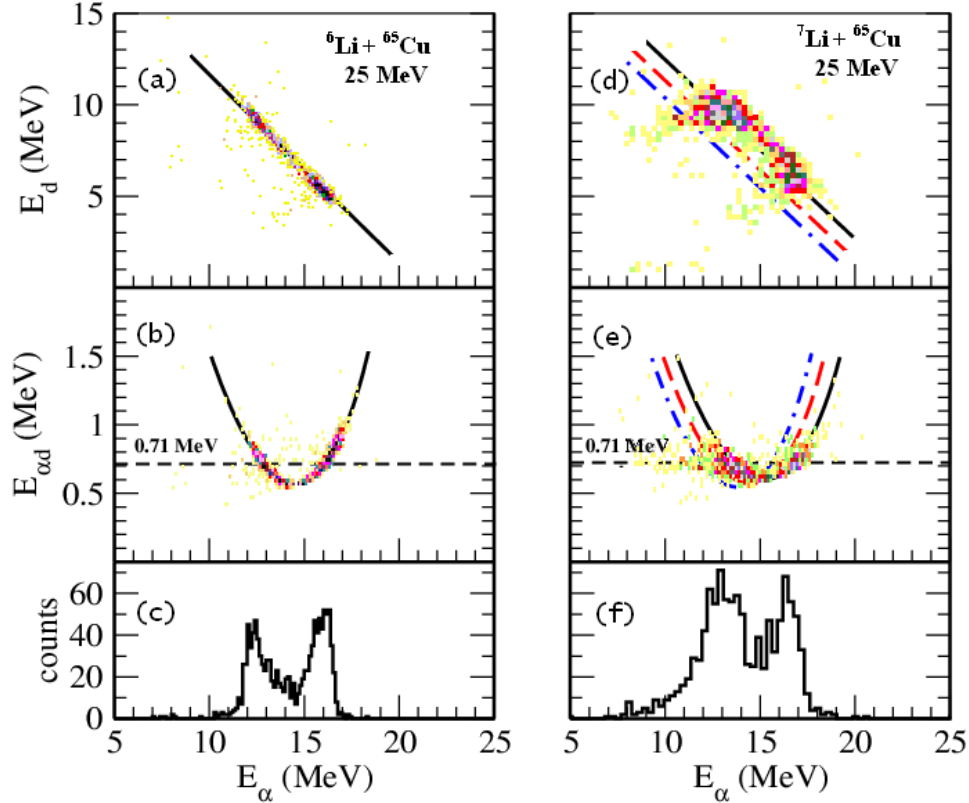


Figure 1. (Color online) Alpha - deuteron correlations for $^{6,7}\text{Li} + ^{65}\text{Cu}$ systems. For the ^6Li projectile the data are for α particles detected at 65° and deuteron at 45° plotted as (a) E_d vs E_α (b) the relative energy $E_{\alpha d}$ vs E_α and (c) projection of the α particle energy for data shown in (b). The solid curves in (a) and (b) are results of three body kinematical calculations. Similar plots for ^7Li projectile for the breakup of $^6\text{Li}^*$ after a $1n$ stripping reaction are shown in (d), (e) and (f) for α particles detected at 26° and deuteron at 46° . The solid, dashed and dot-dashed curves in (d) and (e) are the same as above corresponding to ^{66}Cu in the ground and excited states at 1.15 and 2.14 MeV respectively.

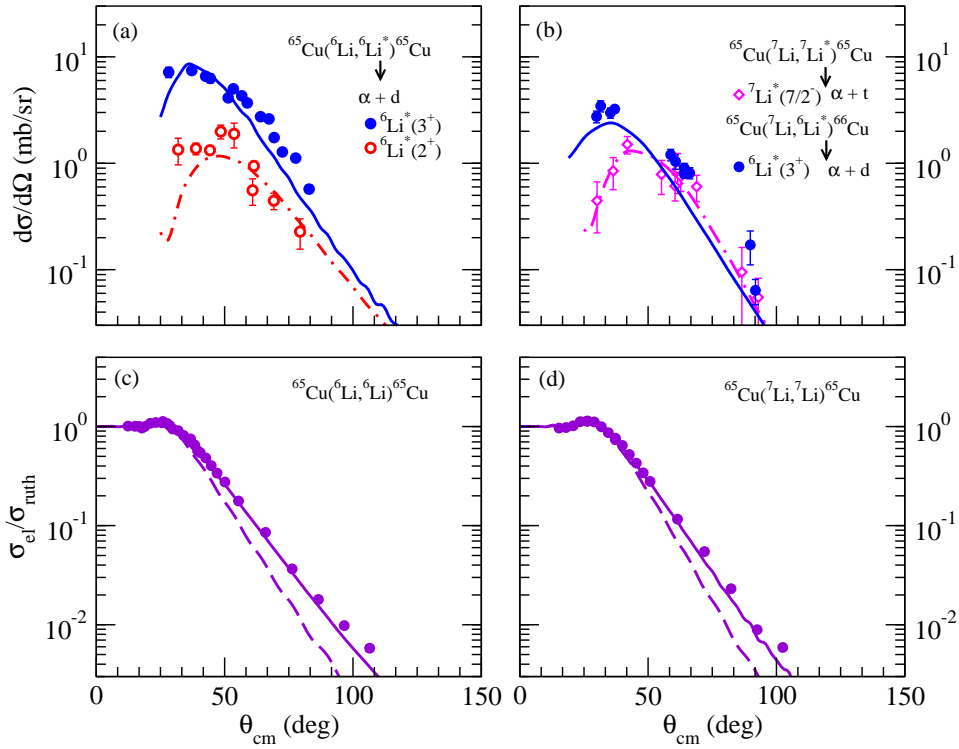


Figure 2. Differential cross-sections for resonant, transfer breakup and elastic scattering. (a) Breakup via resonant states 2.18 MeV (3^+) and 4.31 MeV (2^+) in ^6Li (CDCC calculations are shown as solid and dash-dot lines). (b) Breakup via resonant state 4.63 ($7/2^-$) MeV in ^7Li along with CDCC calculations (dash-dot lines) and data for transfer-breakup reaction, $^7\text{Li} + ^{65}\text{Cu} \rightarrow ^6\text{Li}^*(3^+) + ^{66}\text{Cu}^*$ (0 to 2.5 MeV) along with CCBA calculations. (c) and (d) The ratio of the elastic scattering to the Rutherford cross-section as a function of angle for $^6\text{Li} + ^{65}\text{Cu}$ and $^7\text{Li} + ^{65}\text{Cu}$. CDCC calculations are shown as solid (coupled) and dashed (uncoupled) lines.

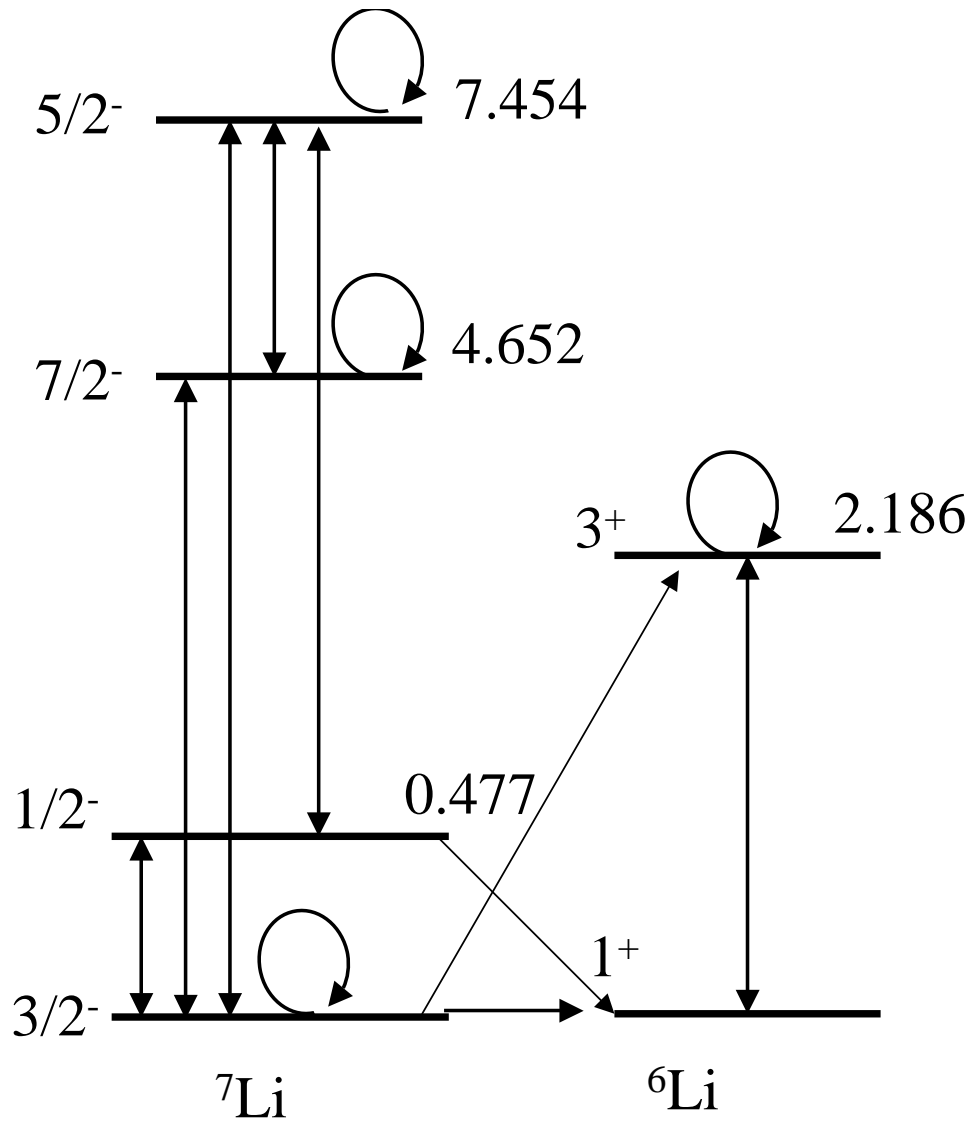


Figure 3. Reduced coupling scheme for the projectile used in the CCBA calculations (see text).